The American Journal of Pathology, Vol. 171, No. 2, August 2007

DOI: 10.2353/ajpath.2007.061092

Cell Injury, Repair, Aging and Apoptosis

Delayed and Deficient Dermal Maturation in Mice Lacking the CXCR3 ELR-Negative CXC Chemokine Receptor

Cecelia C. Yates,* Diana Whaley,* Priya Kulasekeran,* Wayne W. Hancock,† Bao Lu,‡ Richard Bodnar,* Joseph Newsome,* Patricia A. Hebda,§ and Alan Wells*

From the Departments of Pathology, and Otolaryngology,§ University of Pittsburgh and Pittsburgh VAMC, Pittsburgh, Pennsylvania; Millennium Pharmaceuticals, Incorporated,† Cambridge, Massachusetts; and Perlmutter Laboratory,‡ Children's Hospital, Boston, Massachusetts*

Replacement of wounded skin requires the initially florid cellular response to abate and even regress as the dermal layer returns to a relatively paucicellular state. The signals that direct this "stop and return" process have yet to be deciphered. CXCR3 chemokine receptor and its ligand CXCL11/IP-9/I-TAC are expressed by basal keratinocytes and CXCL10/IP-10 by keratinocytes and endothelial cells during wound healing in mice and humans. *In vitro,* these ligands limit motility in dermal fibroblasts and endothelial cells. To examine whether this signaling pathway contributes to wound healing *in vivo*, full-thickness excisional wounds were created on CXCR3 wild-type (+/+) or knockout (−/−) mice. Even at 90 days, long after wound closure, wounds in the CXCR3$^{-/-}$ mice remained hypercellular and presented immature matrix components. The CXCR3$^{-/-}$ mice also presented poor remodeling and reorganization of collagen, which resulted in a weakened healed dermis. This *in vivo* model substantiates our *in vitro* findings that CXCR3 signaling is necessary for inhibition of fibroblast and endothelial cell migration and subsequent redifferentiation of the fibroblasts to a contractile state. These studies establish a pathophysiologic role for CXCR3 and its ligand during wound repair. *(Am J Pathol 2007, 171:484–495; DOI: 10.2353/ajpath.2007.061092)*

Skin wound repair is a complex, highly orchestrated event consisting of an early hypercellular infiltrate that resolves over time, with loss of most of the regenerative-phase dermal fibroblasts and vascular conduits.[1] This reversion of the dermal cellularity is necessary for the maturation and strengthening of the matrix, which when lacking, leads to chronic wounds.[2] This leaves open the question of which signals define both the transition from regeneration to resolution and the cellular involution that accompanies these changes.

Wound repair requires the ordered immigration of fibroblasts into the provisional matrix and keratinocytes over this matrix. This immigration and replacement of the tissue appears to be under the influence of both soluble factors secreted first by platelets and then by inflammatory cell infiltrates, and also matrix components produced by these cells and the immigrated fibroblasts and endothelial cells. Among the latter, tenascin-C and thrombospondins seem to play a major role and thereby mark the immature, regenerative phase of wound healing.[3–5] These influence the functionality of the vasculogenesis by acting, directly or indirectly, through growth factor receptors.[6,7] These events involve a degree of cellular dedifferentiation to enable migration and proliferation. During the remodeling phase, sufficient cells have migrated into the provisional dermal matrix to mature this structure and across the missing epidermal gap to re-establish a keratinocyte covering. These cells then differentiate into synthetic fibroblasts to produce a mature collagen I-rich dermis or basal keratinocytes primed to differentiate vertically. Interestingly, a fully repaired dermis is paucicellular compared with the regenerative phase, implying a significant involution of the stromal support cells (fibroblasts and endothelial cells) present during the regenerative phase.[8] Obviously, late in wound repair, signals must be generated to induce dermal cell differentiation and subsequent cellular loss.

Supported by National Institutes of Health grants GM063569 from the National Institute of General Medical Sciences and HL074597 from the National Heart, Lung, and Blood Institute.

Accepted for publication April 13, 2007.

Address reprint requests to Alan Wells, M.D., DMSc., University of Pittsburgh, Department of Pathology, 3550 Terrace St., Scaife Hall, S-713, Pittsburgh, PA 15261. E-mail: wellsa@upmc.edu.

The nature of such signals is not known. However, a suggestive family of chemokines appears in wounds during late transition to maturation phase. IP-10 (CXCL10) appears in the dermis, being produced by endothelial cells of the neovasculature,[9,10] and IP-9 (CXCL11 or I-TAC) is expressed from redifferentiating keratinocytes behind the leading edge of the wound (Ref. 11 and herein). These secreted peptide factors, both CXC chemokines that lack the canonical N-terminal sequence ELR (glutamic acid-leucine-arginine), bind in common to the ubiquitous CXCR3 chemokine receptor.[12] Signaling through CXCR3 blocks growth factor-induced motility of fibroblasts[11,13] and endothelial cells[14] by suppressing *m*-calpain activation.[15] Interestingly, such a blockade of rear release during motility converts fibroblasts to a contractile behavior,[16,17] reminiscent of the function of these cells during dermal matrix remodeling.[18] Of importance, these chemokines do not block the motility of dedifferentiated keratinocytes but rather increase their motility via lessened adhesiveness[19] and thus would promote more rapid re-epithelialization.[11] Parenthetically, cell homotypic contact inhibition has been proposed as the most likely signal for keratinocyte redifferentiation.[2] The timing of the expression of IP-9 and IP-10, along with their cellular effects, suggests that these chemokines are at least part of the key communication between the dermis and epidermis that signals an end to the regenerative phase and initiation of the remodeling phase of wound repair.

We have shown earlier that keratinocyte-derived IP-9 may act as a soluble paracrine communicator between these compartments.[11] However, although correlative data were present, interventional *in vivo* models were required to demonstrate this role for CXCR3 signaling as a master organizer in wound repair. Mice have been generated that lack CXCR3.[20] These mice displayed decreased immune responsiveness and inflammation in the skin.[20,21] However, wound repair has not been studied in this model system. Thus, we used the CXCR3-null mice to test our hypothesis that, in the absence of CXCR3 signaling, the later resolving phase of wound repair will be impaired and will exhibit a hypercellular, disorganized dermis.

Materials and Methods

Animals

C57BL/6J mice whose CXCR3 expression was abrogated were generated as previously described.[20] In brief, two targeted cell lines were injected into blastocysts derived from C57BL/6 mice. Chimeric males were bred to BALB/c females to yield germline transmission of the targeted allele. Mice were backcrossed at least 6 generations onto the C57BL/6 strain. For this study, $CXCR3^{-/-}$ female mice were bred with $CXCR3^{-/-}$ males, and all offspring were screened for genotype before use. Wild-type C57BL/6J were obtained from Jackson Laboratory. All studies on these animals were performed in compliance with and after approval by the Institutional Animal Care and Use Committees of the Veteran's Administration and University of Pittsburgh. These animals were housed in a facility of Veteran's Affairs Medical Center, Pittsburgh, PA, accredited by the Association for the Assessment and Accreditation of Laboratory Animal Care. Serological analyses did not detect blood-borne pathogens or evidence of infection. Mice were housed in individual cages after wounding and maintained under a 12-hour light/dark cycle in accordance with the guidelines approved by the Institutional Animal Care and Use Committee.

Polymerase Chain Reaction

To verify that the mice were $CXCR3^{-/-}$, genomic DNA from tail clippings was screened by polymerase chain reaction using specific primers for wild-type and $CXCR3^{-/-}$ mice. Three oligonucleotide primers were used. Primer "A" is the forward primer common to both wild-type and $CXCR3^{-/-}$ (5′-CAGGCGCCTTGTTCAACATCAACT-3′). Primer "B" is a reverse primer specific to normal CXCR3 sequence (5′-GTTGTACTGGCAATGGGTGGCATT-3′). Primer "C" is a reverse primer specific to the inserted phosphoglycerate kinase/neomycin sequence and is specific for screening $CXCR3^{-/-}$ mice (5′-ACCTTGCTCCTGCCGAGAAAGTAT-3′). A band size of 239 bp is expected in wild-type DNA, and a band size of 1.1 kb is expected in $CXCR3^{-/-}$ mice. Screenings were further confirmed by sequencing the polymerase chain reaction product inserted in the pCRII vector using M13 forward and reverse sequence primers.

Wounding

Male and female mice (7 to 8 weeks of age, weighing approximately 25 g) were anesthetized with an intraperitoneal injection containing ketamine (75 mg/kg) and xylazine (5 mg/kg). The backs were cleaned, shaved, and treated with 5% povidone-iodine (Betadine; Purdue Products, Stamford, CT) solution. For full-thickness wounds, sharp scissors were used to make an approximately 2-cm diameter circular full-thickness wound through the epidermis and dermis on one side of the dorsal midline; for comparison, the dorsal length of a mouse was about 7.5 cm long. The contralateral uninjured skin served as unwounded control skin. The wounds were covered with liquid occlusive dressing (New-Skin; Medtech, Jackson, WY).[22] This wounding assay was performed three independent times with at least five animals each time.

Wound Contraction

The animals were lightly anesthetized for several seconds. Wounds were traced onto a transparent sheet, at 2-day intervals until complete closure. Wound size was compared between the wild-type and $CXCR3^{-/-}$ groups. The areas described by tracings were measured using Adobe Photoshop image analysis software (version 7.0; Adobe System Inc., San Jose, CA).

Histological Analyses

Mouse

Wound bed biopsies surrounded by a margin of non-wounded skin were collected at days 3, 5, 7, 14, 21, 30, 60, and 90 after wounding. Wound biopsies were fixed in 10% buffered formalin, processed, and embedded in paraffin blocks using standard protocols. Tissue sections (4 μm) were stained with hematoxylin and eosin (H&E) and analyzed for general tissue and cellular morphology. Collagen deposits were evaluated by Masson's trichrome staining.

Dermal Maturation Assessment

Histopathological examination of mouse tissues was performed blinded by a veterinary pathologist. Qualitative assessments were made concerning aspects of dermal and epidermal maturation, inflammation, and granulation tissue. The samples were scored on a scale of 0 to 4 for epidermal healing (0, no migration; 1, partial migration; 2, complete migration with partial keratinization; 3, complete keratinization; and 4, normal epidermis) and dermal healing (0, no healing; 1, inflammatory infiltrate; 2, granulation tissue present–fibroplasias and angiogenesis; 3, collagen deposition replacing granulation tissue >50%; and 4, complete healing). Quantification of fibroblastic hypercellularity was performed by using MetaMorph (Molecular Devices, Downingtown, PA). Cell counting function allowed for the direct counting of dermal nuclei per high-powered field.

Human

Full-thickness 6-mm (open) wounds were made in the skin of the hip region of healthy young adult human volunteers and biopsies taken on days 0, 2, 4, 14, and 28 after wounding. Paraffin tissue sections (5 μm) were stained with hematoxylin and eosin for morphological observations. The original wound studies were approved after full review by the Virginia Commonwealth University/Medical College of Virginia Institutional Review Board, and the use of the specimens herein were deemed exempt by the University of Pittsburgh Institutional Review Board because this tissue was received as excess pathological tissue devoid of protected health information.

Sections for immunohistochemical analysis were incubated with appropriately diluted primary antibody, after antigen retrieval (BioGenex, San Ramon, CA). Antigen staining was performed using diaminobenzidine (Vector Laboratories, Burlingame, CA), then counterstained with Mayer's hematoxylin and coverslipped. In all cases, secondary antibody alone served as a negative control, with various human tumor tissues serving as positive controls.

For mouse tissue, paraffin sections of 4 to 5 μm were prepared for antibody staining. The following antibodies were used for immunohistochemical staining for mouse specimens: CXCR3 (rabbit polyclonal; R&D Systems, Minneapolis, MN), fibronectin (rabbit polyclonal; Rockland, Inc., Gilbertsville, PA), IP-10/CXCL10 (rabbit polyclonal; PeproTech, Rocky Hill, NJ), IP-9/CXCL11 (rabbit polyclonal; PeproTech), tenascin-C (rat polyclonal; R&D Systems), and von Willebrand factor (rabbit polyclonal; Abcam Inc., Cambridge, MA). For murine tissue, antibodies were chosen not to be of murine origin to limit background staining from the secondary antibody. For human specimens, the following primary antibodies were used: CXCR3 (rabbit polyclonal; R&D Systems), IP-9/CXCL11 (goat polyclonal; Santa Cruz Biotechnology, Santa Cruz, CA), and IP-10/CXCL10 (goat polyclonal; Santa Cruz).

Collagen Content

Masson's trichrome staining was used to assess collagen content. Collagen content was assessed using MetaMorph analysis (Molecular Devices). Stained wound biopsies were compared with that of the unwounded controls; at all times the color was maintained to compare the blue- and red-stained areas. The final output was integrated intensity based on total area and staining intensity at individual pixels. All wound biopsies were stained at the same time to eliminate staining variations.

Collagen Alignment and Organization

Picrosirius red staining was used to assess alignment and organization in intact biopsies. Briefly, picric acid (Sigma-Aldrich, St. Louis, MO) was dissolved in 500 ml of distilled water. To this, 0.1 g of Sirius red F3BA was added per 100 ml (Sigma-Aldrich). Paraffin-embedded tissue sections were rehydrated and stained with picric acid. Collagen fibrils were then evaluated by means of polarized light microscopy for both collagen fibril thickness and coherence alignment. Polarization microscopy reveals closely packed thick fibrils of type I collagen fibers as either red-orange intense birefringence in the hypertropic tissue, with thin short loose fibrils as yellow-green. Distribution of fibrils in terms of thickness (cross-sectional area) and arrangement in terms of length of the collagen scars were quantitatively analyzed using MetaMorph (Molecular Devices). Biopsies of unwounded skin served to set the threshold against which the wound biopsies were measured. Percent staining of mature fibers was determined by comparing the total staining intensity of the birefringence (area of staining summed for intensity of pixel) of wound biopsies compared with the biopsies of the contralateral unwounded skin.

Tensile Strength

Biopsies were wrapped flat in foil, snap-frozen in liquid nitrogen, and then stored at −80°C. For the tensile strength measurements, the frozen specimens were divided into two samples, the cross-sectional area measured with calipers, and then the samples were clamped in a custom-built tensiometer and force exerted until wound disruption occurred as previously described.[22]

Measurements were recorded and tensile strength calculated using the formula: maximum tensiometer reading (converted to grams) divided by cross-sectional area (mm^2) = tensile strength (g/mm^2). The results for individual specimens from one wound were combined to determine an average tensile strength per wound. The average tensile strength per wound was tabulated for each group at days 7, 14, 21, 30, 60, and 90 after wounding.

Primary Fibroblast Cultures

Cultures were established from newborn CXCR3$^{-/-}$ and C57BL/6 WT mice. The cells were derived from neonatal mice as previously described.[23] In brief, newborn mice (3 to 4 days old) were euthanized by CO_2 inhalation. The skin was sterilized with povidone-iodine and then ethanol (70%), and then removed from the dorsum and abdomen areas and placed in phosphate-buffered saline plus 2× antibiotics and antimycotics for tissue culture solution for 2 hours. To isolate fibroblasts, the explant method was used in which the skin is cut into small pieces and carefully laid down with the epidermis facing upward in the tissue culture plates. Tissue is allowed to "dry to dampness" before adding Dulbecco's modified Eagle's medium (DMEM) with 10% fetal bovine serum for 4 days to allow cells to migrate from the tissue onto the tissue culture plastic. The cells were characterized as fibroblasts by morphology and immunohistochemistry for vimentin and lack of cytokeratins and CD31. The cells were then incubated in DMEM to allow outgrowth of the fibroblasts. The fibroblasts were used before passage 4.

Cell Migration Assay

Cell migration was assessed by the ability of the cells to move into an acellular area in a two-dimensional wound healing assay. At approximately 70 to 80% confluence, cells were detached and then replated at 1.0×10^5 cells/well in 24-well culture plates in complete growth media (DMEM) and incubated for 24 hours at 37°C in 5% CO_2. Cells were then washed with PBS, and the media were changed to DMEM containing 0.5% dialyzed fetal bovine serum for 24 hours at 37°C in 5% CO_2. A denuded area was generated in the middle of each well with a rubber policeman. The cells were then stimulated with epidermal growth factor (EGF) (10 nmol/L) in the presence or absence of IP-9 (25 ng/ml), adenosine 3′5′-cyclic monophosphorothioate 8-bromo (8-Br-cAMP) (250 nmol/L), adenosine 3′5′-cyclic monophosphorothioate 8-bromo-Rp-isomer (8-Br-Rp-cAMP) (50 nmol/L), or CPT-cAMP (2 μmol/L) and then incubated for 24 hours at 37°C in 5% CO_2. These concentrations were determined empirically to provide either maximum motility or inhibition without toxicity.[13,24] Images were taken at 0 and 24 hours, and the relative distance moved into the wounded area at the acellular front was determined.

Calpain Activity Assay

Calpain activity was determined by using the membrane-permeable substrate t-BOC-Leu-Met-chloromethylaminocoumarin (Boc-LM-CMAC) as described previously.[24] In brief, primary cells were plated at 2.0×10^3 cells/chamber on an eight-well chamber slide (Nalge Nunc International, Rochester, NY) and grown in complete medium for 24 hours. The cells were then incubated in serum-reduced media (0.5% dialyzed fetal bovine serum for DMEM) and incubated for 24 hours. The cells were incubated with 1, 2-bis(2-aminophenoxy)ethane-*N*,*N*,*N*′,*N*′-tetraacetic acid/acetoxymethyl ester (5 μmol/L) for 15 minutes before the addition of Boc-LM-CMAC (50 μmol/L). The cells were further incubated for 15 minutes and then incubated with EGF (10 μmol/L), IP-9 (50 ng/ml), and/or 8-bromo-cAMP (250 μmol/L). The cleavage of Boc-LM-CMAC by calpain was visualized using a fluorescence microscope (Olympus BX40; Olympus, Tokyo, Japan) with a UV blue filter (Olympus MNUA), and images were digitally captured using a SPOT camera and SPOT software (Diagnostic Instruments, Sterling Heights, MI). Images were quantitatively analyzed using MetaMorph (Universal Imaging Corp).

TUNEL Assay

Paraffin sections (5 μm) from each case and time point under investigation were examined for the presence of fragmented DNA in apoptotic cells by the terminal deoxynucleotidyl transferase dUTP nick end labeling (TUNEL) technique using the Roche TUNEL *in situ* staining kit (Roche Molecular Biochemicals, Basel, Switzerland), according to the manufacturer's instructions. To detect DNA fragmentation associated with apoptosis, we used a fluorescence-based TUNEL (false colored red) followed by counterstaining with 4,6-diamidino-2-phenylindole (blue) (Vector Laboratories, Burlingame, CA).

Statistical Analyses

Results are expressed as mean ± SD, and all individual assay measurements were performed in replicate. Statistical differences between groups were determined by the Student's *t*-test. Paired analyses were performed between all groups. Comparisons over time were performed by analysis of variance. Significance was claimed for $P < 0.05$.

Results

CXCR3 Ligands Are Up-Regulated during Wound Healing

The CXCR3 receptor is present on most formed elements of the skin (Figure 1A). *In vitro*, fibroblasts,[13] keratinocytes,[11] and endothelial cells,[14] in addition to cells of the hematopoietic lineage,[12] respond to CXCR3 ligands. Our foundational model, based on cellular effects *in vitro*, posits that the signaling through this receptor depends on timed expression of key ligands. We found differential expression of the CXCR3 ligands IP-9 and IP-10 during wound healing using a mouse model of wound repair. IP-9 was expressed by

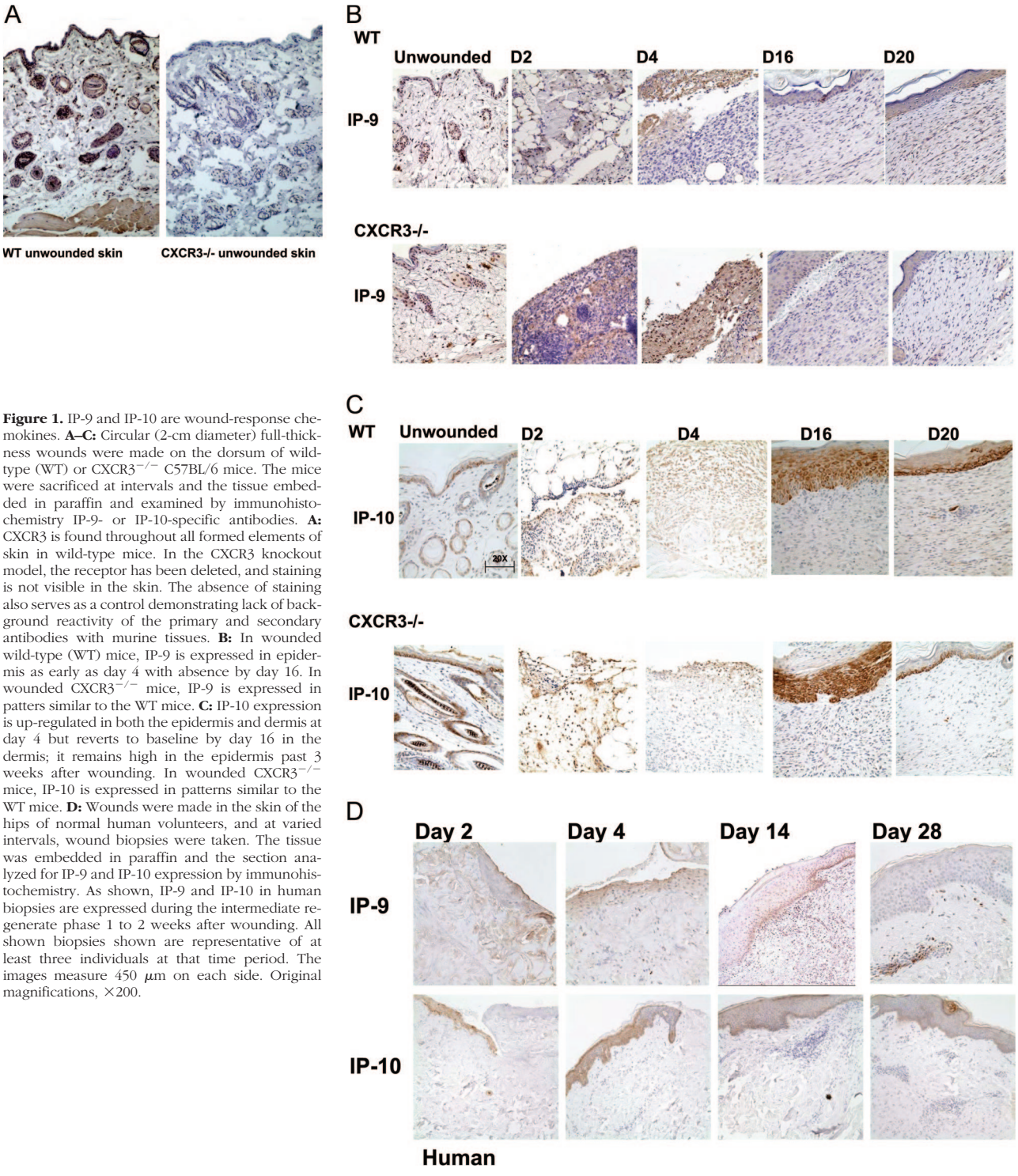

Figure 1. IP-9 and IP-10 are wound-response chemokines. **A–C:** Circular (2-cm diameter) full-thickness wounds were made on the dorsum of wild-type (WT) or CXCR3$^{-/-}$ C57BL/6 mice. The mice were sacrificed at intervals and the tissue embedded in paraffin and examined by immunohistochemistry IP-9- or IP-10-specific antibodies. **A:** CXCR3 is found throughout all formed elements of skin in wild-type mice. In the CXCR3 knockout model, the receptor has been deleted, and staining is not visible in the skin. The absence of staining also serves as a control demonstrating lack of background reactivity of the primary and secondary antibodies with murine tissues. **B:** In wounded wild-type (WT) mice, IP-9 is expressed in epidermis as early as day 4 with absence by day 16. In wounded CXCR3$^{-/-}$ mice, IP-9 is expressed in patters similar to the WT mice. **C:** IP-10 expression is up-regulated in both the epidermis and dermis at day 4 but reverts to baseline by day 16 in the dermis; it remains high in the epidermis past 3 weeks after wounding. In wounded CXCR3$^{-/-}$ mice, IP-10 is expressed in patterns similar to the WT mice. **D:** Wounds were made in the skin of the hips of normal human volunteers, and at varied intervals, wound biopsies were taken. The tissue was embedded in paraffin and the section analyzed for IP-9 and IP-10 expression by immunohistochemistry. As shown, IP-9 and IP-10 in human biopsies are expressed during the intermediate regenerate phase 1 to 2 weeks after wounding. All shown biopsies shown are representative of at least three individuals at that time period. The images measure 450 μm on each side. Original magnifications, $\times$200.

keratinocytes just behind the leading edge of the wound, and IP-10 was expressed deep in the dermis as well as at the wound edge in wild-type mice (Figure 1B for IP-9 and Figure 1C for IP-10). These same results were observed in the CXCR3$^{-/-}$ mice, suggesting that CXCR3 is not required for secretion of its ligands. If anything, there seems to be increased protein levels likely due to lack of receptor-mediated ligand attenuation.

To determine whether the IP-9 and IP-10 expression patterns during mouse wound healing process are relevant to human wound healing, we found that during the healing process in human wounds, IP-9 was expressed during the early granulation phase and IP-10 in the late granulation/early resolving phase (Figure 1D). The results demonstrate a good correlation in IP-9 and IP-10 expression between mouse and human during the wound healing process.

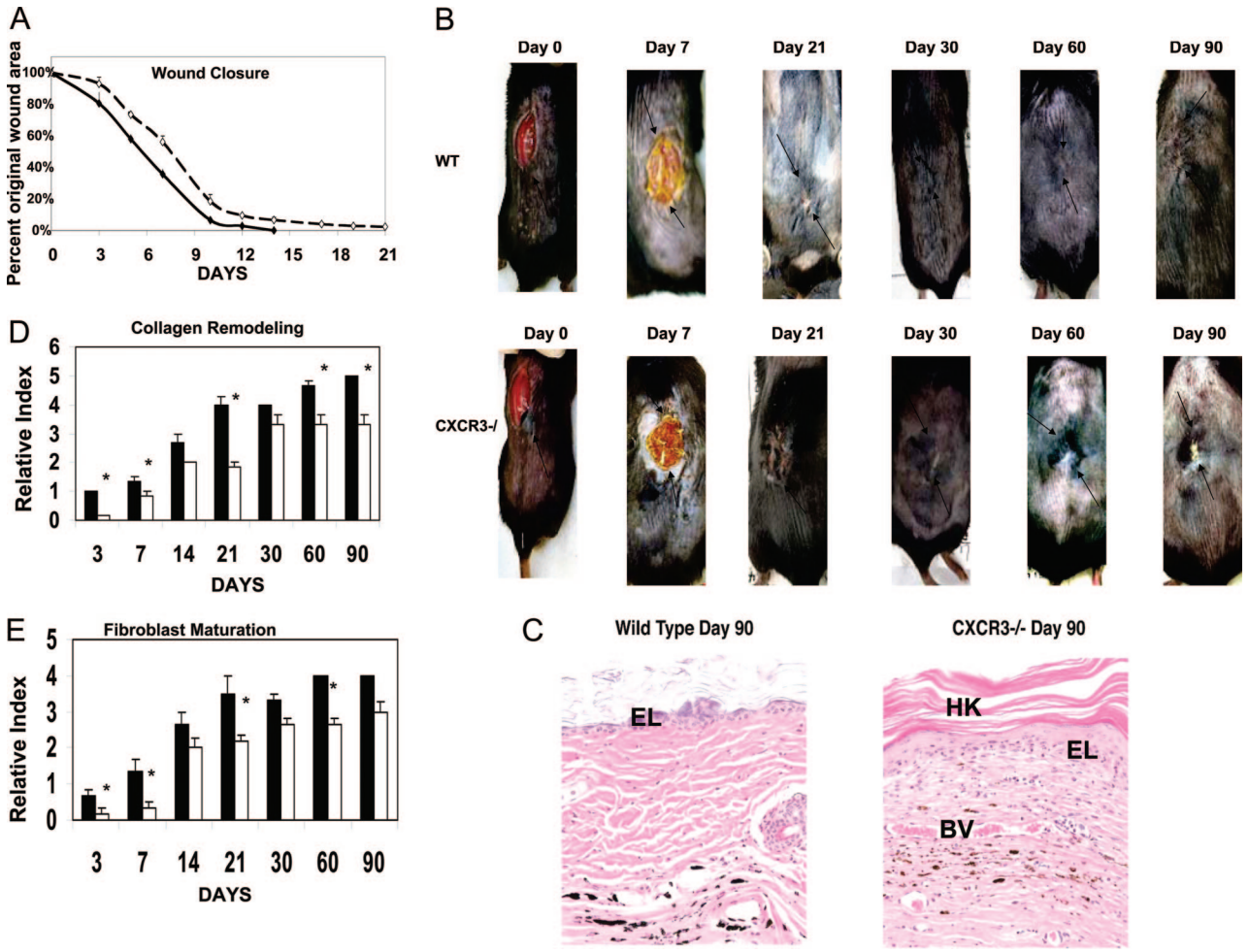

Figure 2. Wound closure is delayed in CXCR3$^{-/-}$ mice. Full-thickness wounds, approximately 2-cm diameter and circular, were analyzed every 2 to 3 days from time 0 until closure. **A:** Wound closure was determined by tracing the wounds and expressing the area relative to initial wound size. Closure of full-thickness wounds was delayed in the CXCR3$^{-/-}$ mice (open diamonds, dashed line) by 2 to 3 days for the rate of closure and up to a week for complete healing when compared with WT mice (filled diamonds, solid line) (mean ± SD, $n = 10$, $P < 0.05$, comparing the wound closure of WT versus CXCR3$^{-/-}$). **B:** CXCR3$^{-/-}$ full-thickness wounds show altered healing patterns. Representative photographs are shown of the full-thickness wounds of various days up to day 90. At day 90, the CXCR3$^{-/-}$ wound showed abnormal healing with a thickened, flaky wound surface shown by **black arrows**, whereas wild-type wounds appeared completely healed. **C:** Histological H&E-stained sections showed that the CXCR3$^{-/-}$ wounds were hyperkeratinized (HK) with a thicker epithelial layer (EL) compared with wild-type wounds even at day 90. The dermis also displayed hypercellularity (HC) at day 90 in the CXCR3$^{-/-}$ mice. **D** and **E:** Histological assessments were made of each wound at all time points by a blinded veterinary pathologist. Collagen remodeling was determined by the alignment of the collagen fibrils; fibroblast infiltration in the wounded area was determined by scoring the maturity of the fibroblast from most reactive to normal. WT mice are shown as black bars, CXC3R$^{-/-}$ as open bars. Measurements were made on a scale of 0 to 5 (unwounded) (mean ± SD, $n = 3$, $^*P < 0.05$ comparing WT versus CXCR3$^{-/-}$). In **B** and **C**, the pictures and histological sections were representative of three individual mice. The **black marks** are from the India ink used to delineate the original wound. The photomicrographs measure 300 μm on each side. Original magnifications, ×400.

Lack of CXCR3 Delays Dermal Wound Healing

Once we had a system in which CXCR3 signaling is present or absent in skin, we asked whether this paracrine signaling system, which we have previously shown *in vitro* is necessary for the inhibition of fibroblast motility and induction of a contractile state,[11] functions *in vivo*. Circular (2 cm in diameter) full-thickness wounds were made by removing the epidermal and dermal layers of the skin on the backs of mice. These wounds healed in both genotypes, but there was a greater than 2-day lag in the closure rate for the CXCR3$^{-/-}$ mice, with full closure occurring a week later on average (Figure 2A; $n = 10$; $P < 0.05$). Since full-thickness wounds in mice close predominantly via contraction, this delay was consistent with the *in vitro* mechanism of CXCR3 signaling channeling dermal fibroblasts from migration to contraction.[16]

The delay in full-thickness wound healing was evident by day 7 in the CXCR3$^{-/-}$ mice compared with the wild-type mice (Figure 2A). However, after an extended time period, the abnormality in healing of full-thickness wounds became more grossly apparent (Figure 2B). Even after 3 months, the CXCR3$^{-/-}$ wounds presented what appeared to be a scab because of its flaky appear-

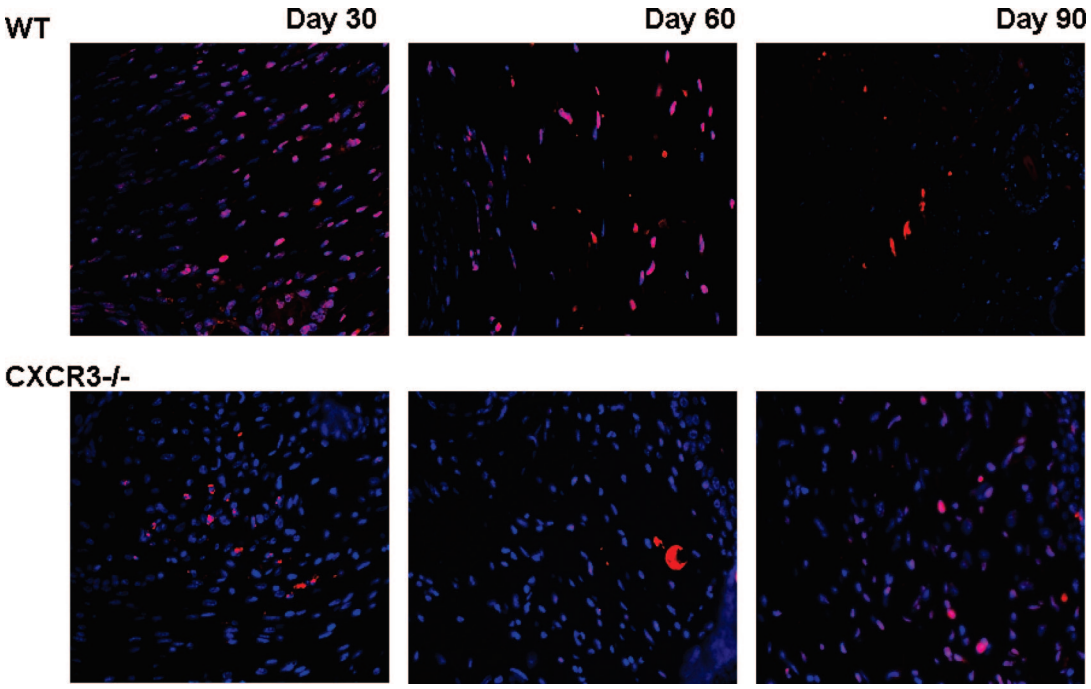

Figure 3. Apoptosis of dermal cells is delayed in mice lacking CXCR3. Apoptosis was assessed in CXCR3$^{-/-}$ mice by *in situ* TUNEL throughout the healing process. Representative micrographs ($n = 3$ for each mouse genotype per time point) show apoptotic signaling determined by DNA fragmentation associated with apoptosis. Detection of apoptotic cells (red) showed fewer apoptotic events in wounds in the CXCR3$^{-/-}$ mice than in the wild-type mice; nuclei are stained by 4,6-diamidino-2-phenylindole stain (blue). These stains were merged resulting in a violet stain for apoptotic cells; red alone is considered nonspecific.

ance. Histological examination of these day-21-to-90 wounds revealed a thicker epithelial layer and prominent thick and hypercellular stratum corneum (hyperkeratinization), seemingly less well connected to the dermis as late as day 90 (Figure 2C). Histologically, examination of the biopsies presented an immature hypercellular dermis

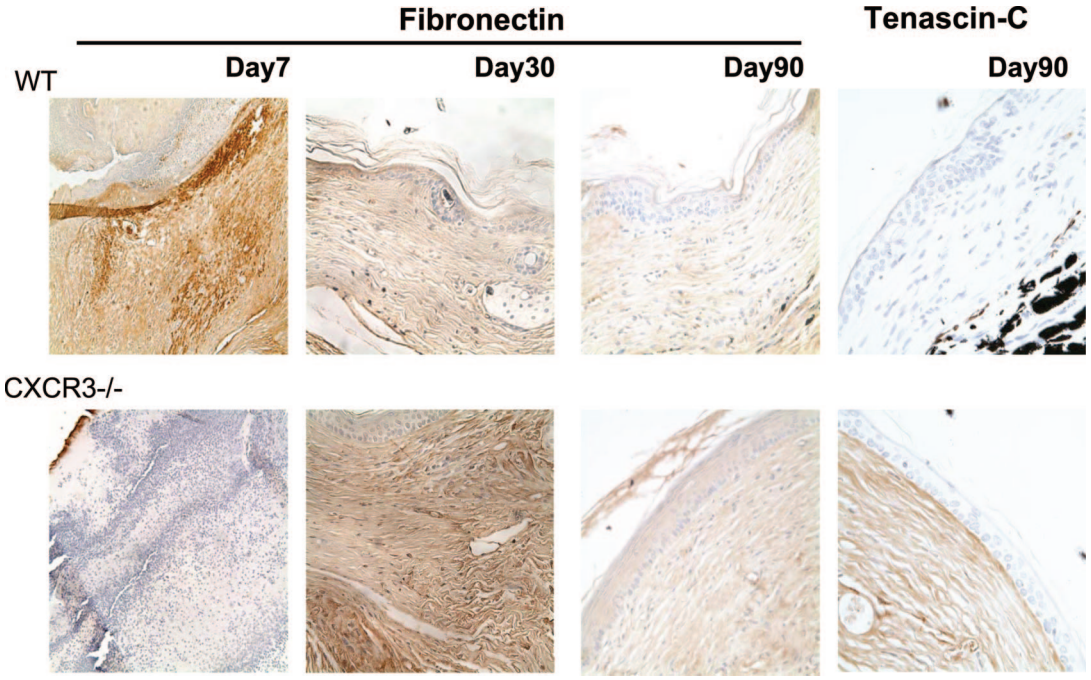

Figure 4. Wound immaturity of CXCR3$^{-/-}$ is reflected in the persistent presence of tenascin and fibronectin. Tenascin-C becomes pronounced on day 2 in both wild-type and CXCR3$^{-/-}$ wounds (data not shown). As the scar develops and matures, tenascin expression decreases in the wild-type wound, yet in the CXCR3$^{-/-}$, strong wound expression is still present as late as day 90. There also is an enhanced expression of fibronectin in the CXCR3$^{-/-}$ wound compared with the wild-type wounds at day 60, with even somewhat elevated levels at day 90. Interestingly, fibronectin expression in wounds of the CXCR3$^{-/-}$ mice seems to be delayed since it is still absent from day 7, although present by day 14 (data not shown). Shown are representative of three wounds in each mouse variant. The images measure 200 μm on each side. Original magnifications, $\times$400.

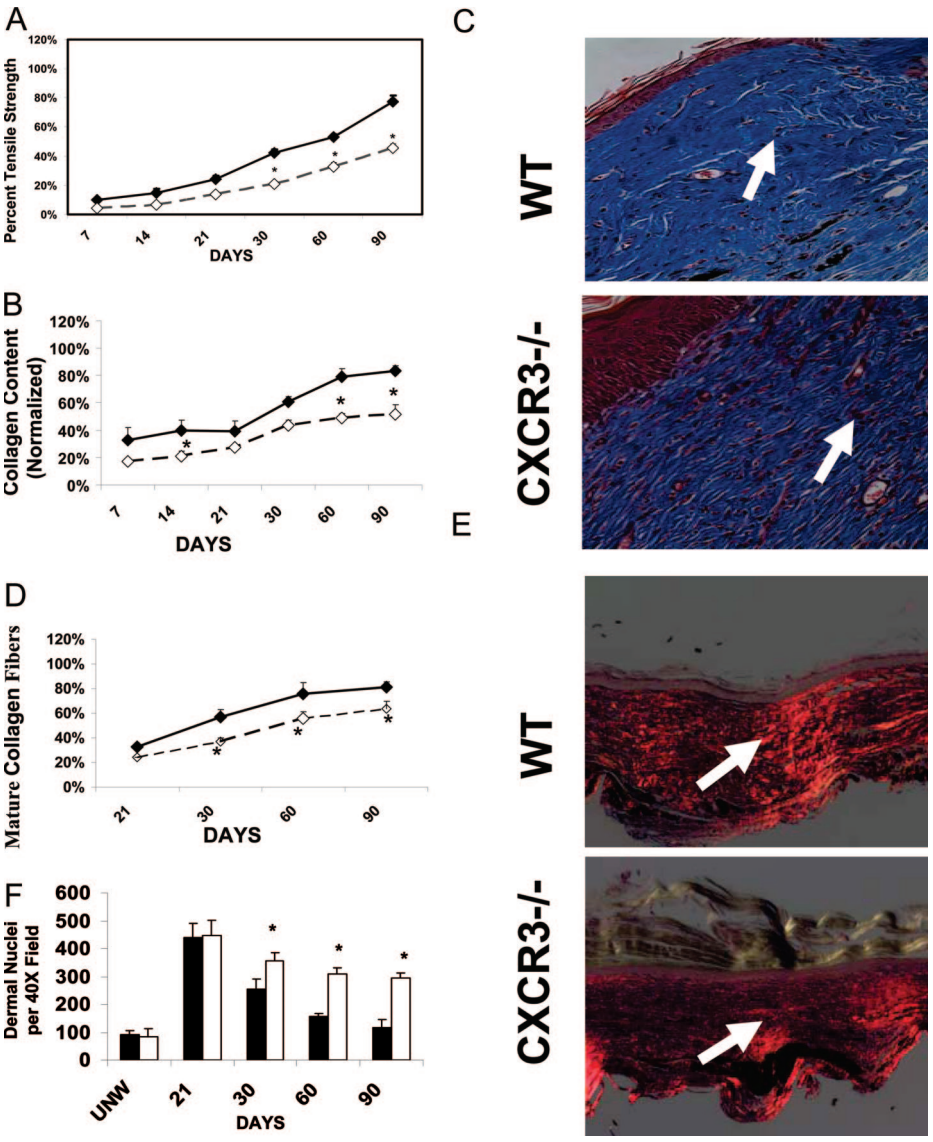

Figure 5. Lack of CXCR3 results in a weakened wound dermis. **A:** Full-thickness wounds surrounding normal skins biopsies were taken from the CXCR3$^{-/-}$ (open diamonds, dashed line) and wild-type (filled diamonds, solid line) mice at days 7 to 90 after wounding for tensile strength measurements. The CXCR3$^{-/-}$ wounds showed significantly less tensile strength than the wild-type wounds at days 30 and beyond (mean ± SD, n = 6,*$P < 0.05$). **B–E:** The CXCR3 wounds contained less collagen, and what was present was poorly organized. **B** and **C:** Collagen was quantified using Masson's trichrome staining. Images of the CXCR3$^{-/-}$ and wild-type wounds showed distinguishable patterns of collagen remodeling. MetaMorph analysis of the wound collagen confirmed that the CXCR3$^{-/-}$ wounds had significantly less collagen than wild-type wounds at days 60 and 90 (shown), as shown by **arrows** (mean ± SD, n = 3, *$P < 0.05$). **D** and **E:** Quantitative analysis of collagen alignment showed a significant difference between the wild-type and CXCR3$^{-/-}$ wounds at days 30 and 90 (shown). Picrosirius red staining showed that healing of the CXCR3$^{-/-}$ full-thickness wounds results in less organized dermal matrix, shorter collagen fibers, and an immature scar, as shown by **arrows** (determined by total integrated birefringence compared with contralateral unwounded skin; mean ± SD, n = 3, *$P < 0.05$). **F:** CXCR3$^{-/-}$ wounds (open bars) remained hypercellular as late as 90 days after wounding compared with WT wounds (solid bars) and unwounded skin (UNW) (mean ± SD, n = 3, *$P < 0.05$). The images measure 300 μm on each side. Original magnifications, ×400.

(Figure 2C) and was quantified (Figure 2, D and E) as was predicted by our model that CXCR3 signaling serves as an "off" signal for wound healing.

Wounds in Mice Lacking CXCR3 Signaling Presented Delayed Apoptosis of Dermal Cells

The exuberant cellularity that marks the regenerative phase is reversed during wound resolution. Thus, the noted hypercellularity months after wounding and even wound closure may correspond to a deficit in this regression. We probed for a marker of apoptotic cell death, free ends indicative of DNA fragmentation in these wounds (Figure 3). TUNEL staining of the wound field biopsies demonstrated that 30 and 60 days after wound healing, there was a significantly greater absolute and relative number of apoptotic cells in the dermis in the wounds of wild-type mice compared with CXCR3$^{-/-}$ mice. However, by day 90, at which time point the healed wounds in wild-type mice are paucicellular, dermal cell apoptosis continued in the wound fields of the CXCR3$^{-/-}$ mice. This suggests the CXCR3 signaling is at least in part responsible for the cell apoptosis during the resolving phase that restores a paucicellular dermis.

Matrix Immaturity in the Absence of CXCR3 Signaling

One of the defining aspects of mature skin is the maturation of the matrix to allow for a basement membrane delineating the dermal-epidermal separation. This transition from immature matrix to delineating margin is marked by progression from expression of fibronectin and tenascin-C to laminin V and collagen IV by both dermal fibroblasts and epithelial keratinocytes.[25,26] In the absence of the CXCR3 signaling, the progression to a mature matrix and a remodeled basement membrane seemed retarded (Figure 4). Staining for provisional matrix components tenascin-C and fibronectin showed a persistence of the transient tenascin-C expression even through 90 days.

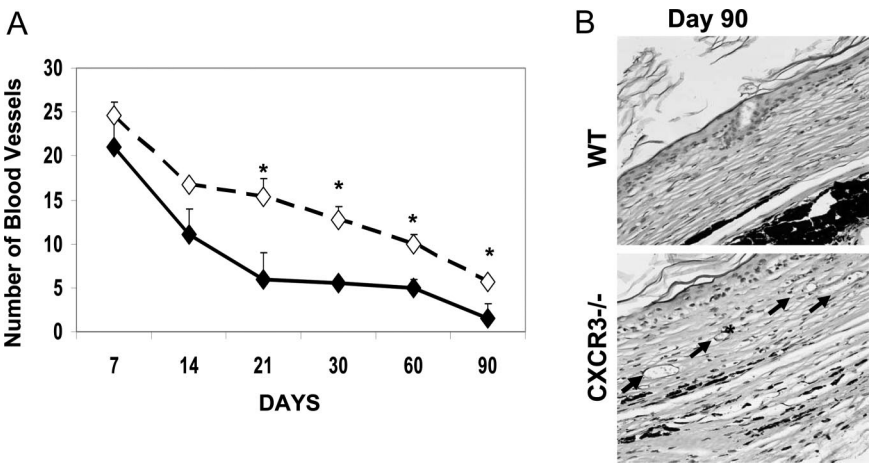

Figure 6. Blood vessels persist in the wounds or mice lacking CXCR3. Neovascularization in CXCR3$^{-/-}$ mice was assessed using immunostaining of von Willebrand factor antigen outlining blood vessels of the mice. **A:** Quantitation of the number of capillaries, as determined by von Willebrand factor staining and morphometry, with a low-power field in the center of the wound is shown in the graph. WT mice are represented by filled diamonds with solid line, and CXCR3$^{-/-}$ are represented by open diamonds with dashed line. This was derived from two independent experiments of three mice in each group/time period ($n = 6$) with each mouse evaluated in three random low-power fields (shown are mean ± SD, $^*P < 0.05$). **B:** Representative von Willebrand factor immunostaining demonstrates the paucity of capillaries (**arrows**) at day 90 in wild-type wound compared with the CXCR3$^{-/-}$ wounds. The images measure 300 μm on each side. Original magnifications, ×400.

The reactive fibronectin expression seemed to be delayed, only appearing after 7 days, and being quite pronounced at 60 days, although returning to normal by day 90. These changes were noted both throughout the dermis and in the area that should form the basement membrane barrier in the CXCR3$^{-/-}$ wounds.

Deficient Collagen Organization and Dermal Wound Strength

A major function of the fibroplasia after wounding is to regenerate the collagen matrix of the dermis. However, it is only after the fibroblasts are channeled toward a "differentiated" state that they become synthetic.[27] In addition, it has been speculated that myofibroblast contraction of the matrix is required for collagen bundling and alignment during the remodeling phase of wound repair.[16,28,29] Thus, we asked whether the CXCR3$^{-/-}$ mice presented a weakened dermis. Tensiometry demonstrated that in unwounded skin, CXCR3$^{-/-}$ mice presented somewhat higher absolute tensile strength (31 ± 6% increased) than that of wild-type mice. However, during wound healing, the regain of tensile strength of the CXCR3$^{-/-}$ mice wounds lagged behind that of wild-type mice, and even at 90 days after wounding, the CXCR3$^{-/-}$ mice regained only 40 to 50% of the prewounding strength compared with 70 to 80% for the wild-type mice (Figure 5A). Even when comparing absolute tensile strength, the wounds in the CXCR3$^{-/-}$ mice were still significantly less strong than those of the wild-type mice at all time points measured (71 ± 10% of wild type, $P < 0.01$).

To determine whether this difference in regained tensile strength between the wild-type and CXCR3$^{-/-}$ wounds is due to collagen content and organization, histological analyses were undertaken. Masson's trichrome staining showed less collagen in the CXCR3$^{-/-}$ wounds from days 7 through 90 (Figure 5, B and C). In addition, the wild-type wounds displayed a denser and more organized granulation tissue at day 90, suggesting better healing of these wounds (Figure 5, C and E). Picrosirius red staining showed that in the wounds of CXCR3$^{-/-}$ mice, the collagen fibers were short and the scar immature (Figure 5, D and E). Histological assessment of the hematoxylin and eosin-stained sections also detected an immaturity in the collagen of the dermal matrix (Figure 2C). Interestingly, this collagen deficiency was not due to a paucity of fibroblasts; the CXCR3$^{-/-}$ mice presented a significantly hypercellular wound dermal compartments at day 90 (Figure 5F). This is consistent with CXCR3 activation being a "stop immigration" signal. Interestingly, by day 90, when the wild-type wounds were well past the regenerative stage, the CXCR3$^{-/-}$ wounds were still hyperkeratinized, hypercellular, and contained a significantly greater density and/or number of blood vessels.

Angiogenic Response Is Persistent in the Absence of CXCR3 Signaling

ELR-negative CXC chemokines have been thought to regulate the angiogenic drive during wound healing by inhibiting the growth and migration of proliferating endothelial cells.[14] CXCR3 receptor expression is increased during the inflammatory phase after day 4 and suppresses uncontrolled angiogenesis.[30] We had predicted that in the absence of the receptor, a proangiogenic state would appear throughout all stages of repair (Figure 6A). The knockout mice showed an up-regulated angiogenic response compared with wild type even at day 90 (Figure 6B), suggesting that the CXCR3 receptor contributes to the timing and regulation of vascularization, which may in turn aid in homeostasis during wound healing.

Fibroblasts Lacking CXCR3 Respond to Growth Factor Stimulation

A central cell type implicated in this model is the dermal fibroblast, which normally expresses CXCR3. It is possible that in the CXCR3-null mice, these fibroblasts are deficient in signaling elements in addition to CXCR3 itself. As we have shown previously *in vitro* that fibroblast migration was inhibited by IP-9 and IP-10 through a protein kinase A (PKA) inhibition of *m*-calpain,[13,15] we focused on these two elements, the inte-

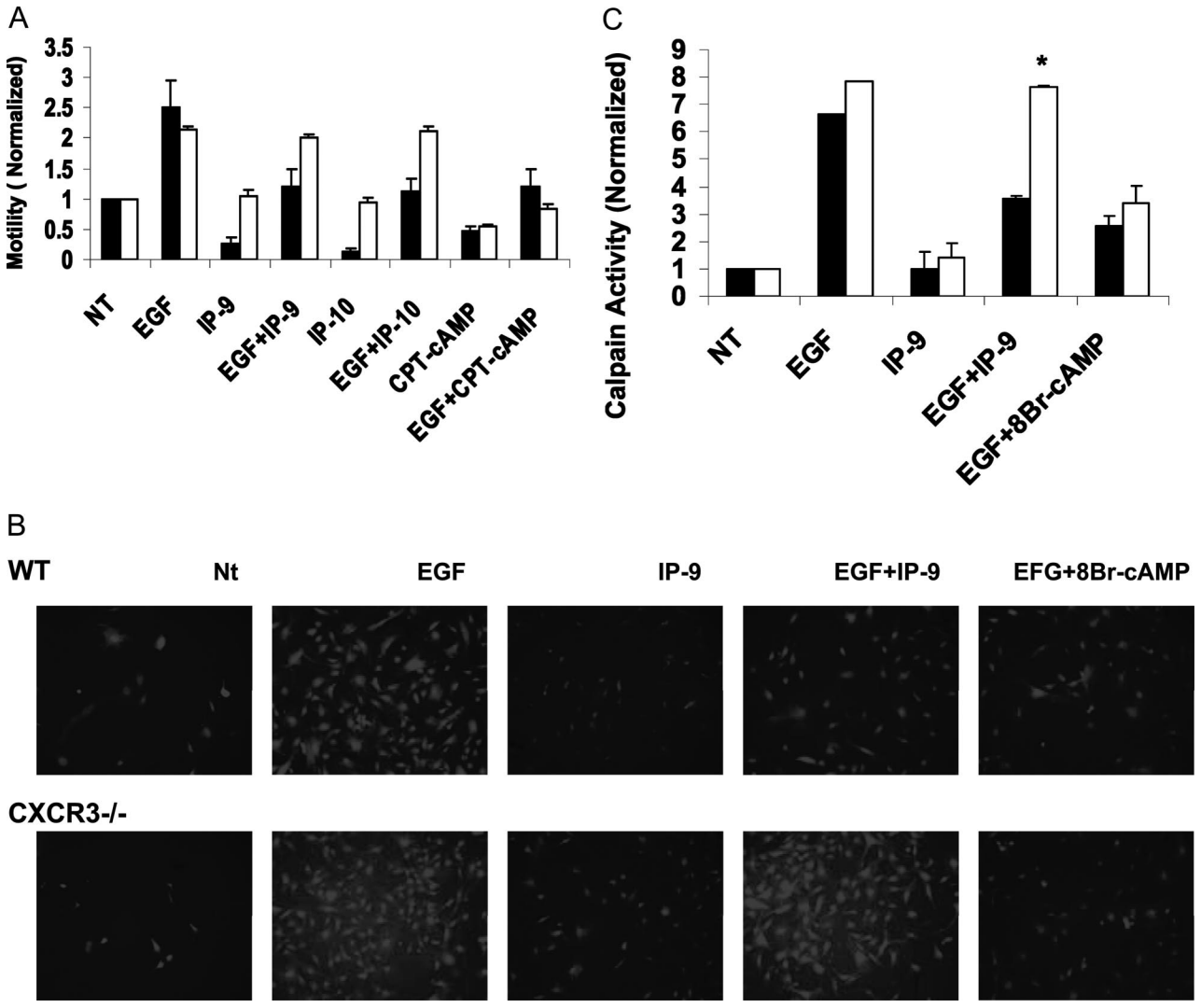

Figure 7. Dermal fibroblasts from CXCR3-null mice appear normally responsive with the exception of CXCR3 signaling. Primary dermal fibroblasts were isolated from wild-type and CXCR3$^{-/-}$ mice and analyzed for response to a wound growth factor (EGF for the EGF receptor network) and the CXCR3 ligands. **A:** In a two-dimensional *in vitro* "wound healing" assay, fibroblasts from both mice were equally responsive to EGF, but only the wild-type dermal fibroblasts responded to IP-9. Fibroblast cells were grown to ~80 to 85% confluence in a 12-well plate and quiesced in 0.5% dialyzed fetal bovine serum DMEM for 24 hours. A 1-mm-wide "scratch wound" was made in the fibroblasts monolayer using a rubber policeman. The cells were then incubated in 0.5% dialyzed DMEM alone (NT) (no treatment) or containing EGF (10 nmol/L) in the presence or absence of IP-9 (25 ng/ml) or IP-10 (200 ng/ml) and/or the membrane-permeant PKA activator CPT-cAMP (2 μmol/L). As expected, IP-9 and IP-10 inhibited motility only in the wild-type fibroblasts, but by bypassing CXCR3 signaling and directly activating PKA, both types of fibroblasts were limited in their migratory capacity and EGF response (mean ± SD, $n = 3$, $P < 0.05$ comparing the wild-type to CXCR3$^{-/-}$ fibroblasts in response to IP-9 or IP-10). **B:** To demonstrate that this failure to inhibit motility involved the well-described blockade of calpain activation, fibroblasts were plated on gelatin-coated glass chamber slides at 1.0×10^4 cells/well and incubated for 24 hours and then further incubated in 0.5% dialyzed fetal bovine serum DMEM for 24 hours. The cells were preincubated with or without 1,2-bis(2-aminophenoxy)ethane-*N,N,N′,N′*-tetraacetic acid/acetoxymethyl ester (50 μmol/L) and/or the PKA activator 8-Br-cAMP (250 μmol/L) before treatment with EGF (10 μmol/L) and/or IP-9 (50 ng/ml) in the presence of Boc-LM-CMAC (27 μmol/L). Calpain activation was analyzed by fluorescence microscopy. Fluorescence within the cell indicates calpain activity. 8-Br-cAMP was able to inhibit EGF-mediated *m*-calpain activation in both wild-type and CXCR3$^{-/-}$ fibroblast explants. **C:** Calpain activity was quantified by MetaMorph analysis (mean ± SD, $n = 6$). IP-9 only inhibited *m*-calpain activation in wild-type fibroblasts. WT mice are shown as black bars, CXC3R$^{-/-}$ as open bars. *$P < 0.05$. Data shown are from a representative experiment of three, each with a different cell isolate.

grated response of motility and the molecular event of *m*-calpain activation. We isolated fibroblasts from wild-type and CXCR3$^{-/-}$ mice. Both primary dermal fibroblasts migrated in response to EGF, but only wild-type fibroblast locomotion was limited by IP-9 and IP-10 (Figure 7A). This failure to block rear release was reflected in the ability of IP-9 to prevent EGF-initiated activation of calpain in the CXCR3$^{-/-}$ fibroblasts (Figure 7, B and C). That the CXCR3-null fibroblasts were only lacking the CXCR3 triggering of PKA inhibition of calpain was shown by CPT-cAMP being able to block migration of these cells similar to wild-type cells (Figure 7A). These cells were also similar to wild-type cells in EGF-induced proliferation (data not shown), which was unaffected by CXCR3 ligands as expected.[13]

Discussion

Wound healing is essential for the survival of any organism. Failure to heal properly leads to chronic wounds (venous, diabetic, and pressure ulcers), infection, meta-

bolic derangements, or excessive healing and its concomitant scarring. Proper healing requires not only sufficient repopulation of the missing tissue but also subsequent maturation of the nascent wound bed. For skin, the initial regenerative phase with significant dermal cellularity undergoes dermal matrix production, maturation, and cellular involution as part of this last remodeling phase of wound healing. The studies herein shed some light on the understudied question of how the different components of skin end their regenerative phase to form a mature tissue during the wound resolution phase. Our foundational model has soluble factors working through the common receptor for ELR-negative chemokines, CXCR3, which channels the dermal elements toward a paucicellular and relatively avascular organized collagen-rich matrix similar to unwounded skin. In mice lacking this CXCR3 receptor, the fibroplasia and angiogenic responses seem to persist with a resulting hypercellular dermis that has less collagen and, even accounting for this deficit, fewer mature fibers thereof. This results in a weakened dermis.

A caveat to these studies relates to our lack of negating CXCR3 signaling by an independent method. This is an unfortunate consequence of the nature of the signaling network and proposed role that CXCR3 plays later in wound resolution. First, because CXCR3 ligands are multiple, eliminating only one would not be expected to recapitulate the deletion of the common receptor. Still, we have initiated efforts to parse the contributions of at least epidermally derived IP-9 during skin repair; however, such studies lie beyond the scope of the present communication. Second, blockade of CXCR3 signaling is possible using antibodies. This was not attempted because the initial findings in the CXCR3-null mice suggested that the major role was later in the resolving phase of wound repair, with actions through 3 months. Thus, this intervention was precluded by considerations of the technical issues of antibody delivery into the dermal matrix without inducing an antibody-mediated immune response that would impinge on the wound healing.

Furthermore, we have discussed throughout the CXCR3 ligands IP-9/CXCL11 and IP-10/CXCL10 as the relevant ones for the wound healing defects noted herein. The importance of these two ligands is inferred because of their presence during the regenerative and resolving phases of wound healing.[10,11] However, the other two CXCR3 ligands, PF4/CXCL4 and MIG/CXCL9, likely play roles, albeit at earlier time points since these ligands arise mainly from platelets and macrophages, respectively.[21,30] Although there are reports of these ligands modulating angiogenesis, among other wound aspects, the temporal nature of their appearance argues against a role in the deficiencies of later dermal maturation focused on herein. However, studies that lie beyond the scope of the current manuscript are investigating these more acute actions.

It must be noted that although the wound repair in mice lacking CXCR3 is deficient, it does occur and thus seems to be mainly a temporal deficit rather than an absolute qualitative omission. The mice lacking CXCR3 did close their wounds and regained skin structures and function, although at delayed times. As such, there exist redundancies in wound repair pathways, as would be expected for a response so critical to animal survival. What these other, possibly compensatory, pathways may be remain to be determined. However, it is possible that these other pathways are operative during development because the CXCR3$^{-/-}$ mice develop seemingly normal skin, almost indistinguishable from wild-type mice before wounding (the CXCR3$^{-/-}$ mice skin is slightly thicker in our observations). Thus, the wound phenotype, at least in the CXCR3$^{-/-}$ mice, seems to recapitulate the ontogeny of skin development, further supporting the concept that wound repair actuates a replay of the embryonic/fetal mechanisms of development.

The wounds in the CXCR3-null mice presented a hypercellular dermis. This may be due to failure either in preventing immigration and/or proliferation or in inducing apoptosis or a combination thereof. It is unlikely that this outcome is due to a defect in fibroblast proliferation, since IP-10 had no effect on induced proliferation of human dermal fibroblasts *in vitro*[13] or in the explanted cells herein. Furthermore, *in vitro*, the CXCR3 ligands did not induce fibroblast death; however, it remains to be determined whether these chemokines predispose or potentiate fibroblast and endothelial cell apoptosis from other signals derived from the resident inflammatory cells. The most likely failure is that of permitting persistent fibroblast immigration into the wound bed from surrounding tissue. CXCR3 ligands block growth factor-induced locomotion by preventing *m*-calpain-mediated rear release.[15] This not only limits migration but channels the transcellular contractility toward matrix compaction[16,17] a process critical for dermal maturation.[28,29] Of interest, this chemokine signaling pathway may also alter the differentiation status of these fibroblasts. Despite having a surfeit of fibroblasts, the dermis is lacking in collagen content and density. Whereas the deficit in collagen bundles may be related to the necessity of contraction for generating such, the diminished amount of collagen is even more striking when considered on a per-fibroblast basis. Thus, it is likely that the CXCR3 signaling cascades actuate fibroblast differentiation into a synthetic cell; this is currently being investigated.

The role of CXCR3 signaling in epidermal repair is still emerging. Initial observations suggest a delay in re-epithelialization and even thickened epidermal cell and keratin layers. However, these observations require extensive and separate experimentation that lies beyond the current manuscript. Germane to these studies, the progression from provisional matrix to mature matrix and a formed basement membrane that delineates and separates the mature dermal and epidermal layers seems to be retarded, with markers of provisional matrix still prominent at days 60 and 90 in wounds of the CXCR3$^{-/-}$ mice. Although it is true that keratinocytes actually contribute substantially, if not predominantly to this basement membrane,[31] fibroblast immaturity in the CXCR3$^{-/-}$ mice might delay the formation of a mature basement membrane even in the absence of keratinocyte deficiencies. As such, further investigation is necessary to address this question.

All of these findings have intriguing implications for rational interventions aimed at promoting wound healing or limiting scarring. What is attractive is that this signaling axis involves extracellular factors that are accessible for either removal/blockade or augmentation. Thus, disrupting CXCR3 signaling should lead to less collagen and fewer bundles, with limited scarring. On the other hand, additional CXCR3 signaling, via a ligand applicant, may result in more rapid maturation of the skin compartments. Last, and most speculatively, it has not escaped our notice that the wound repair in the $CXCR3^{-/-}$ mice bears a resemblance to that noted during keloid dysplasia, with a hypercellular dermis and thickened epidermis.

Acknowledgments

We thank Diane George, Anand Krishnan V. Iyer, Sourabh Kharait, Vlad Sandulache, Latha Satish, and Clayton Yates for providing suggestions and discussions. Services in kind were provided by the Pittsburgh VA Medical Center.

References

1. Clark RAF: Epithelial-mesenchymal networks in wounds: a hierarchical view. J Invest Dermatol 2003, 120:ix–xi
2. Jaffe AT, Heymann WR, Lawrence N: Epidermal maturation arrest. Dermatol Surg 1999, 25:900–903
3. Harty M, Neff AW, King MW, Mescher AL: Regeneration or scarring: an immunologic perspective. Dev Dyn 2003, 226:268–279
4. Midwood KS, Schwarzbauer JE: Tenascin-C modulates matrix contraction via focal adhesion kinase- and rho-mediated signaling pathways. Mol Biol Cell 2002, 13:3601–3613
5. Esemuede N, Lee T, Pierre-Paul D, Sumpio BE, Gahtan V: The role of thrombospondin-1 in human disease. J Surg Res 2004, 122:135–142
6. Swindle CS, Tran K, Johnson TD, Banerjee P, Mayes AM, Griffith LG, Wells A: Epidermal growth factor (EGF)-like repeats of human tenascin-C as ligands for EGF receptor. J Cell Biol 2001, 154:459–468
7. Kellouche S, Mourah S, Bonnefoy A, Schoevaert D, Podgorniak MP, Calvo F, Hoylaerts MF, Legrand C, Dosquet C: Platelets, thrombospondin, and human dermal fibroblasts cooperate for stimulation of endothelial cell tubulogenesis through VEGF and PAI-1 regulation. Exp Cell Res 2007, 313:486–499
8. Gailit J, Clark RAF: Wound repair in the context of extracellular matrix. Curr Opin Cell Biol 1994, 6:717–725
9. Luster AD, Greenberg SM, Leder P: The IP-10 chemokine binds to a specific cell surface heparan sulfate site shared with platelet factor 4 and inhibits endothelial cell proliferation. J Exp Med 1995, 182:219–231
10. Strieter RM, Kunkel SL, Arenberg DA, Burdick MD, Polverini PJ: Interferon γ-inducible protein 10 (IP-10), a member of the C-X-C chemokine family, is an inhibitor of angiogenesis. Biochem Biophys Res Commun 1995, 210:51–57
11. Satish L, Yager D, Wells A: ELR-negative CXC chemokine IP-9 as a mediator of epidermal-dermal communication during wound repair. J Invest Dermatol 2003, 120:1110–1117
12. Romagnani P, Maggi L, Mazzinghi B, Cosmi L, Lasagni L, Liotta F, Lazzeri E, Angeli R, Rotondi M, Fili L, Parronchi P, Serio M, Maggi E, Romagnani S, Annunziato F: CXCR3-mediated opposite effects of CXCL10 and CXCL4 on TH1 or TH2 cytokine production. J Allergy Clin Immunol 2005, 116:1372–1379
13. Shiraha H, Gupta K, Glading A, Wells A: IP-10 inhibits epidermal growth factor-induced motility by decreasing epidermal growth factor receptor-mediated calpain activity. J Cell Biol 1999, 146:243–253
14. Bodnar R, Yates C, Wells A: IP-10 blocks VEGF-induced endothelial cell motility and tube formation via inhibition of calpain. Circ Res 2006, 98:617–625
15. Shiraha H, Glading A, Chou J, Jia Z, Wells A: Activation of m-calpain (calpain II) by epidermal growth factor is limited by PKA phosphorylation of m-calpain. Mol Cell Biol 2002, 22:2716–2727
16. Allen FD, Asnes CF, Chang P, Elson EL, Lauffenburger DA, Wells A: EGF-induced matrix contraction is modulated by calpain. Wound Repair Regen 2002, 10:67–76
17. Smith KD, Wells A, Lauffenburger DA: Multiple signaling pathways mediate compaction of the collagen matrices by EGF-stimulated fibroblasts. Exp Cell Res 2006, 312:1970–1982
18. Grinnell F, Ho C-H, Tamariz E, Lee DJ, Skuta G: Dendritic fibroblasts in three-dimensional collagen matrices. Mol Biol Cell 2003, 14:384–395
19. Satish L, Blair HC, Glading A, Wells A: IP-9 (CXCL11) induced cell motility in keratinocytes requires calcium flux-dependent activation of μ-calpain. Mol Cell Biol 2005, 25:1922–1941
20. Hancock WW, Lu B, Gao W, Csizmadia V, Faia K, King JA, Smiley ST, Ling M, Gerard NP, Gerard C: Requirement of the chemokine receptor CXCR3 for acute allograft rejection. J Exp Med 2000, 192:1515–1520
21. Liu L, Callahan MK, Huang D, Ransohoff RM: Chemokine receptor CXCR3: an unexpected enigma. Curr Top Dev Biol 2005, 68:149–181
22. Hebda PA, Whaley DL, Kim H-G, Wells A: Absence of inhibition of cutaneous wound healing in mice by oral doxycycline. Wound Repair Regen 2003, 11:373–379
23. Devalaraja RM, Du J, Qian Q, Yu Y, Devalaraja MN, Richmond A: Delayed wound healing in CXCR2 knockout mice. J Invest Dermatol 2000, 115:234–244
24. Glading A, Chang P, Lauffenburger DA, Wells A: Epidermal growth factor receptor activation of calpain is required for fibroblast motility and occurs via an ERK/MAP kinase signaling pathway. J Biol Chem 2000, 275:2390–2398
25. Larjava H, Salo T, Haapasalmi K, Kramer RH, Heino J: Expression of integrins and basement membrane components by wound keratinocytes. J Clin Invest 1993, 92:1425–1435
26. Mackie EJ, Liverani D: Induction of tenascin in healing wounds. J Cell Biol 1988, 107:2757–2767
27. Reed MJ, Vernon BB, Abrass IB, Sage EH: TGF-β1 induces the expression of type I collagen and SPARC, and enhances contraction of collagen gels, by fibroblasts from young and aged donors. J Cell Physiol 1994, 158:169–179
28. Grinnell F: Fibroblasts, myofibroblasts, and wound contraction. J Cell Biol 1994, 124:401–404
29. Grinnell F, Ho CH, Skuta G: Differences in the regulation of fibroblast contraction of floating versus stressed collagen matrices. J Biol Chem 1999, 274:918–923
30. Romagnani P, Lasagni L, Annunziato F, Serio M, Romagnani S: CXC chemokines: the regulatory link between inflammation and angiogenesis. Trends Immunol 2004, 25:201–209
31. Usui ML, Mansbridge JN, Muffley LA, Carter WG, Olerud JE: Morphological evidence for the role of suprabasal keratinocytes in wound reepithelialization. Wound Repair Regen 2005, 13:468–479